Nonlinear Dyn (2022) 108:1–14
https://doi.org/10.1007/s11071-021-07165-w

FEATURE ARTICLE

Dynamics of circular oscillator arrays subjected to noise

Balakumar Balachandran · **Thomas Breunung** · **Gizem D. Acar** · **Abdulrahman Alofi** · **James A. Yorke**

Received: 25 October 2021 / Accepted: 20 December 2021 / Published online: 30 January 2022

Abstract Energy localization, which are spatially confined response patterns, have been observed in turbomachinery applications, micro-electromechanical systems, and atomic crystals. While confined energy can reduce a device's life-span, in sensing and energy harvesting applications, it can be beneficial to steer a system's response into a localized mode. Building on earlier studies, in this article, the authors extend the research on localization by considering an array of coupled Duffing oscillators arranged in a circle. The system is composed of multiple nonlinear oscillators each connected to two neighboring oscillators via springs. Due to the periodic boundary conditions waves can propagate through the boundaries. These oscillators are hardening in most of the considered cases, and softening in the others. In the studied parameter range, the system is characterized by multi-stable behavior and a localized mode as well as a unison-low-amplitude motion coexist. The possibility that white noise can drive the system response from the localized mode to the low amplitude mode and thus suppresses energy localization is investigated. For different noise levels, the duration needed to stop energy localization as well as the probability to suppress localization within a certain time is numerically studied. In addition, the effects of linear coupling and nonlinear coupling between the oscillators on the strength of localization and the minimum noise addition needed to suppress energy localization are examined in depth. Moreover, modeling of large array dynamics with smaller subsystems is explored and dynamics with non-Gaussian noise is also considered.

Keywords Circular arrays · Duffing oscillators · Energy localization · Noise

B. Balachandran (✉) · T. Breunung · A. Alofi
Department of Mechanical Engineering, University of Maryland, College Park, MD 20742, USA
e-mail: balab@umd.edu

G. D. Acar
Department of Mechanical Engineering, Stevens Institute of Technology, Hoboken, NJ 07030, USA

J. A. Yorke
Department of Mathematics, University of Maryland, College Park, MD 20742, USA

1 Introduction

Energy localization is a response state, in which energy exchange between sub-elements (oscillators) of a system can lead the system's energy to be spatially focused in one or a few of the sub-elements (oscillators). This response localization has been found to occur in systems with defects or imperfections [1] and homogeneous lattices with nonlinearities and discreteness [2]. Energy localization can occur during transient dynamics [3] or steady-state dynamics. Localized modes have been found to occur in nonlinear oscillator arrays, including cyclically symmetric rotational systems [4] and micro-resonator arrays [5].

Suppression of energy localization is important for many mechanical systems, as this localization can lead to structural failures of machinery parts due to the localized high amplitude (high energy) oscillations. For other applications, such as for energy harvesting or sensing, focusing the system's energy in a certain sub-element may be desirable. Understanding the mechanisms leading to energy localization and nonlinear analyses to identify localized modes are helpful to develop strategies to suppress or spatially move a localization.

Although breathers in a homogeneous continuum can pass through each other without exchanging energy, in discrete lattices, the energy of breathers may add up when they collide, which results in localization of the energy [6]. Nonlinear discrete systems with weak coupling can exhibit energy localization, in which energy can build up in a single sub-element without diffusion to the neighboring sub-elements. Localized modes often exist in frequency ranges where multiple solution branches exist [7]. Depending on the initial conditions, the system's oscillatory response may be on a different solution branch even when the harmonic forcing is the same. Systems with multi-stable behavior can be driven from one solution to another by perturbing the oscillation through addition of noise to the harmonic forcing. For a single Duffing oscillator with a double potential well, Agarwal et al. [8] showed that by applying Gaussian noise, the system response can be driven from one solution branch to another or in some cases, the multi-stable behavior can be eliminated, and the system response can be similar to that of a linear oscillator. Perkins et al. [9] studied the influence of Gaussian noise on intrinsic localized modes of a nonlinear oscillator array with free-free boundary conditions. For this system, they showed that energy localization can be suppressed with noise. In this system, each of the oscillators is coupled with two of its neighbors, except the first and the last one, where propagating waves reflect from the boundaries. In this work, localized modes in a circular configuration of six to twenty coupled Duffing oscillators is studied. The system has periodic boundary conditions, and each oscillator is coupled to its left and right neighbors, and waves can propagate through the boundaries without interruptions.

For an array of hardening Duffing oscillators with periodic boundary conditions subjected to a harmonic excitation, Papangelo et al. [7] studied different response branches. They showed that the system response has multi-stability characteristics in certain frequency regions, where depending on the initial conditions, the array can oscillate in either a unison-amplitude mode or an energy localized state. They also pointed out that the localized modes exist only when the forcing is above a certain level. When the system is excited with a low forcing, the system exhibits linear system like behavior, and energy localization is not observed. A similar system is studied here and Gaussian and non-Gaussian noise is utilized to move the system response from the localized mode to a uniform-low-amplitude (ULA)mode.

In this work, white Gaussian noise is used to perturb the system when it is in a energy localized state, and push the system response out of the basin of attraction of the localized mode. Then, the noise addition is removed, and the system response is found to be attracted to the ULA mode in steady state. A dynamic noise duration algorithm is applied, wherein the noise application is continued until the localized oscillator's amplitude drops below a certain level (i.e., the trajectory moves out of the basin of attraction of the localized mode). Then, this noise application is stopped. The system then settles in a state of ULA oscillations. The system response is studied for a number of noise levels, by using hundreds of different noise vectors, and the duration required to suppress the localization is recorded for each simulation. The system's response to noise is studied in an averaged sense, and the probability of localization suppression is investigated for different noise levels and simulation lengths. In addition, the effects of the inter-oscillator coupling on the localization suppression are explored. The minimum noise level needed to suppress localization is studied for systems with both linear coupling stiffness and nonlinear coupling stiffness. Moreover, similarities between the responses of small arrays and large arrays are investigated. If similarities are present, this can help in reduction of the computational costs and allow one to understand the localization behavior in a large array by simulating only a system comprised of the localization center and a few adjacent neighbors. This study is concluded by comparing the influence of non-Gaussian noise models on energy localization with the observations for Gaussian noise obtained in the preceding sections.

The rest of the paper is organized as follows. In the next section, a description of the system is given with a calculation of localized modes. Then, in the subsequent section, the effects of Gaussian noise on sys-

tem response is discussed through numerical simulations, where the duration needed for the noise to suppress localization is calculated, the effect of coupling is explored, and the studies are extended to large arrays and non-Gaussian noise models. Concluding remarks are presented at the end.

2 System description and localized modes

The oscillatory system of interest is sketched out in Fig. 1. It is composed of identical Duffing oscillators with linear springs and cubic springs, and these oscillators are arranged in a cyclically symmetric layout. The oscillators are coupled through linear and nonlinear springs, where the coupling springs are weak compared to the oscillator stiffness k. The system is excited with a harmonic excitation.

Assuming each oscillator has mass $m = 1$, mass normalized equations of motion of a coupled oscillator array with periodic boundary conditions can be written as

$$\ddot{x}_n + c\dot{x}_n + k_1 x_n + k_3 x_n^3 + f_c(x_n) = F_0 \cos(\omega t), \quad (1)$$

for $n = 1, 2, \ldots N$, where c is the damping, k_1 is the linear stiffness, k_3 is the cubic stiffness, and f_c is the coupling spring force with $f_c(x_n) = k_c(2x_n - x_{n-1} - x_{n+1}) + k_{c3}[(x_n - x_{n+1})^3 + (x_n - x_{n-1})^3]$ for $1 < n < N$, $f_c(x_1) = k_c(2x_1 - x_N - x_2) + k_{c3}[(x_1 - x_2)^3 + (x_1 - x_N)^3]$ and $f_c(x_N) = k_c(2x_N - x_{N-1} - x_1) + k_{c3}[(x_N - x_1)^3 + (x_N - x_{N-1})^3]$. Depending on the signs of k_1 and k_3, each individual oscillator can behave as either a monostable or a bistable oscillator, and can have hardening or softening characteristics. In this study, an array of primarily, hardening Duffing oscillators (with $k_1 > 0$ and $k_3 > 0$) are considered.

Papangelo et al. [7] showed that an energy localized mode exists for the selected parameters $k_1 = 1, k_3 = 1$, $c = 0.01$, $k_c = 0.04$, and $k_{c3} = 0$, when the system is harmonically excited with the forcing parameters being $F_0 = 0.0126$ and $\omega = 1.25$. When oscillating in this configuration, one of the oscillators has a significantly larger amplitude compared to the other ones. To capture this mode numerically, the anti-continuous method [10] was used. The localized mode is first found at the anti-continuous limit; that is, uncoupled limit (for the system with $k_c = 0$ and $k_{c3} = 0$). In this limit, for a single oscillator's response state, there are two stable periodic orbits, one with a low-amplitude and another

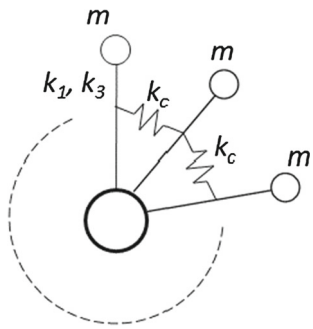

Fig. 1 A circular array of coupled Duffing oscillators with periodic boundary conditions

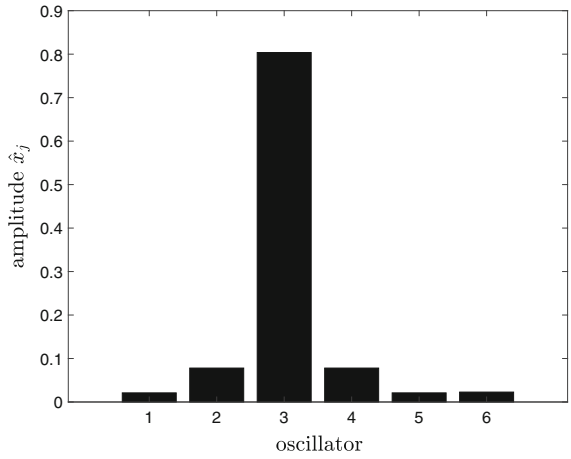

Fig. 2 The amplitude profile for the localized mode with coupling spring stiffness $k_c = 0.04$

with a high amplitude. Thus, for the full N-mass array, stable periodic orbits exist, which continue to exist for low enough coupling stiffness. These modes can be computed with standard continuation techniques (e.g., [11]) or with the automated continuation package COCO [12], which has been employed in this article.

Here, the authors focus on the mode, where the third mass oscillates with high amplitude, while the other oscillators remain at a relatively low vibration level. An amplitude $\hat{x}_j$ is defined as the maximal absolute displacement of the j-th oscillator along a stable periodic steady-state solution, for example, the localized mode. The amplitude profile of the oscillators for the localized mode is given in Fig. 2, when the nonlinear coupling is absent. The energy is localized in the third oscillator, whereas the other oscillators have much lower amplitudes. The amplitude profile is symmetric about the localized oscillator. It is noted that due to cyclic sym-

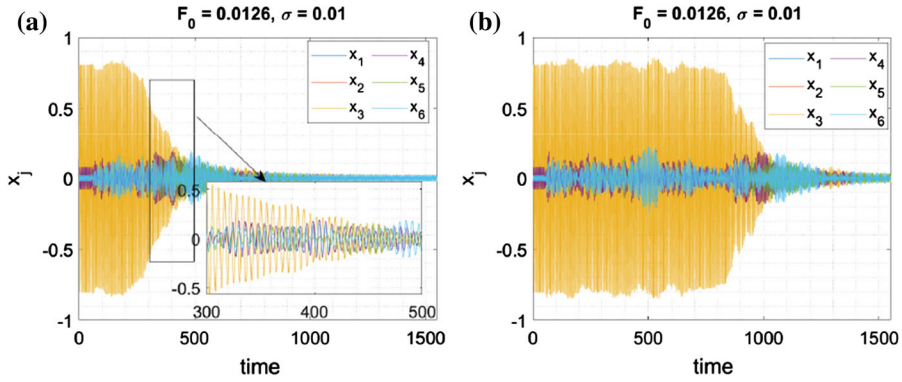

Fig. 3 Time histories of the oscillator responses: Before the noise is applied, energy localization occurs in the third oscillator, while the other oscillators move with smaller amplitudes. Upon application of the Gaussian noise, the energy localization disappears and the solution moves from the localized mode to the ULA mode. Two different noise realizations are used in cases (a) and (b). The time noise takes to suppress the localization is different for the two cases

metry localized modes with maximal energy in any of the other oscillators exists as well.

In the next section, Gaussian noise is added to perturb the system response from the localized mode. The authors investigate whether the noise can successfully destroy the energy localization.

3 Noise induced suppression of energy localizations

In order to explore the effects of white Gaussian noise on the localized mode, and to investigate if the noise can be used to suppress the energy localization, a Gaussian noise term is added to the right-hand side of Eq. (1), yielding

$$\ddot{x}_n + c\dot{x}_n + k_1 x_n + k_3 x_n^3 + f_c(x_n) = F_0 \cos(\omega t) + \sigma \dot{W}(t), \tag{2}$$

where σ is the intensity of the white Gaussian noise, $W(t)$ is a Wiener process and $\dot{W}(t)$ is a mnemonic derivative. To ensure the uniformity in forcing, the authors assume the same noise term is applied to all of the oscillators. Throughout this work, the non-dimensional parameters values are given by

$$k_1 = 1, \quad k_3 = 1, \quad \omega = 1.25, \quad F_0 = 0.0126,$$

which correspond to the values from reference [7]. The linear coupling spring stiffness k_c, the nonlinear coupling spring stiffness k_{c3}, and the noise intensity σ are varied. The stochastic equations of motion (2) can be represented in state space form as

$$\begin{aligned} \dot{x}_{n1} &= x_{n2}, \\ \dot{x}_{n2} &= F_0 \cos(\omega t) + \sigma \dot{W} - c x_{n2} - k_1 x_{n1} - k_3 x_{n1}^3 \\ &\quad - f_c(x_{n1}). \end{aligned} \tag{3}$$

Stochastic differential equations are more appropriately addressed in differential form yielding

$$\begin{aligned} dx_{n1} &= x_{n2} dt, \\ dx_{n2} &= (F_0 \cos(\omega t) - c x_{n2} - k_1 x_{n1} - k_3 x_{n1}^3 \\ &\quad - f_c(x_{n1}))dt + \sigma dW. \end{aligned} \tag{4}$$

The term dW indicates the differential of the noise term. Detailed treatments of stochastic differential equations can be found in references [13,14]. In this work, the equations of motion (4) are integrated by using the Euler–Maruyama scheme [15].

For a system with six oscillators, the localized mode can be destroyed by noise, as the time series of the system response for $\sigma = 0.01$ shown in Fig. 3a reveal. In this example, the system is forced with harmonic forcing only for the first 250 s. Oscillator 3 moves with a much larger amplitude compared to the other ones (i.e., the system's energy is localized in oscillator 3). At t = 250s, in addition to the harmonic forcing, a Gaussian noise with intensity $\sigma = 0.01$ is applied to the system. The oscillator's response is noisy, but stays around the localized mode for a while. Then, around t = 400s, the response is found to depart from the localized mode and move to the ULA mode. The noise addition is removed from the forcing around t = 1000 s, and the resulting

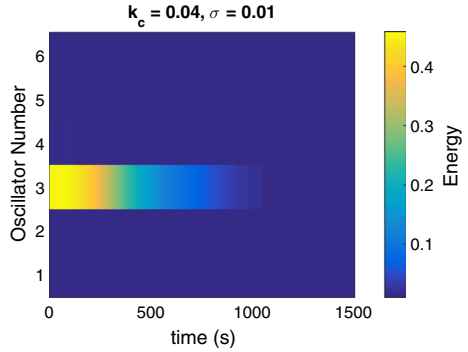

Fig. 4 Energy distribution of the oscillators averaged for 400 noise vectors: The energy is localized in the third oscillator in the beginning. The Gaussian noise is found to suppress localization, leading to a uniform, low-amplitude response

response is found to remain in the ULA mode. For the same noise level, but for a different realization of the stochastic process, the duration until the system reaches the ULA mode differs (from around t = 550 s in Fig. 3a), as shown in Fig. 3b.

3.1 The effect of noise intensity

In order to explore the effects of the noise intensity, Monte-Carlo simulations are carried out for which the system is studied with 400 different noise vectors with the same intensity, and the average behavior of the array is investigated. The time it takes for noise to suppress energy localization is compared for different noise levels. Naturally, it is expected that a large noise intensity would initiate the collapse faster.

For a noise intensity of $\sigma = 0.01$, the system is simulated with 400 different noise vectors. The averaged energy distribution of the system is given in Fig. 4, where the noise added to the system can suppress the localization. Although from each simulation, it is found that the noise level $\sigma = 0.01$ is sufficient to destroy the localized mode, the duration needed to do so is found to be different for different noise vectors.

The numerical simulations are extended to lower noise levels. In Fig. 5, averaged energy distribution across the oscillators are shown for the noise intensities $\sigma = 0.008$ and $\sigma = 0.006$. For each noise level, the energy of each oscillator is averaged over 400 simulations with different noise vectors of the same intensity. In both cases, the noise level is found to be sufficient to suppress the localization, although, it takes longer for the suppression to be initiated at the lower noise intensities ($\sigma = 0.008$ and $\sigma = 0.006$).

To systematically calculate the duration needed to apply the noise to suppress energy localization, a dynamic noise application algorithm is used as shown in Fig. 6. The system is initialized at the localized mode at time $t = 0$. Then, the equations of motion (4) are integrated for one period and the distance between the sample and the ULA mode is calculated. If this distance is less than a tolerance tol, the system is close to the ULA mode. Hence, the response has departed from the localized mode. In this case the localization has been successfully suppressed and the integration is terminated. If the system is not close to the ULA mode, then the integration is continued. The tolerance tol was set to be half of the distance between the localized mode and ULA mode.

The probability of suppression of energy localization within a given time as a function of the noise intensity is shown in Fig. 7. For each noise level one hundred realizations were computed. From Fig. 7, it can be discerned that the likelihood of a successful suppression of localization by noise increases with the duration of noise application as well as with the noise intensity. This could imply that if one can waits "long enough," there is a possibility that even the smallest amount of noise can add up and suppress energy localization. Although, the localized mode is stable, as the noise perturbs the system, the attraction of the stable mode is overcome by the random perturbations.

Indeed, according to the theoretical results on randomly perturbed dynamical systems by Freidlin and Wentzell [16] or Matkowsky and Schuss [17], any trajectory of system (4) will leave the basin of attraction of the localized mode for any noise intensity $\sigma \neq 0$. Moreover, the mean time for such an exit will grow exponentially as the noise intensity σ approaches zero. Therefore, one can search for a practical noise limit that is sufficient to suppress localizations in a "reasonable" amount of time.

3.2 Effect of inter-oscillator coupling

The effects of coupling between the oscillators on the localized modes was studied in [18], where it was shown that it is "easier" to create energy localization with random initial conditions when the coupling is low. For arrays with stronger coupling, more energy can

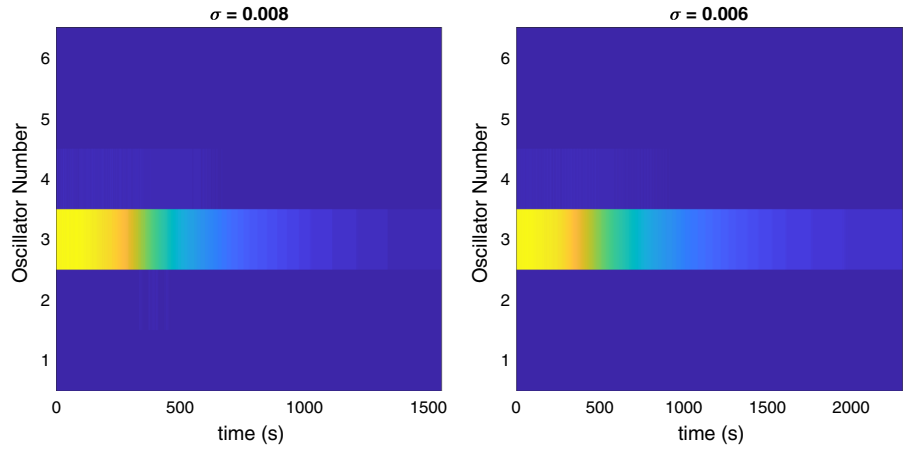

Fig. 5 Energy distribution of the oscillators averaged for 400 noise vectors for $\sigma = 0.008$ and $\sigma = 0.006$: The energy is localized in the third oscillator in the beginning. Gaussian noise addition has been used to suppress localization, leading to a uniform, low-amplitude response

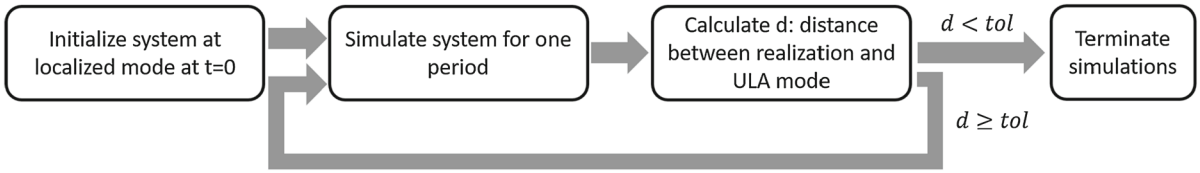

Fig. 6 Steps in the dynamic noise duration algorithm

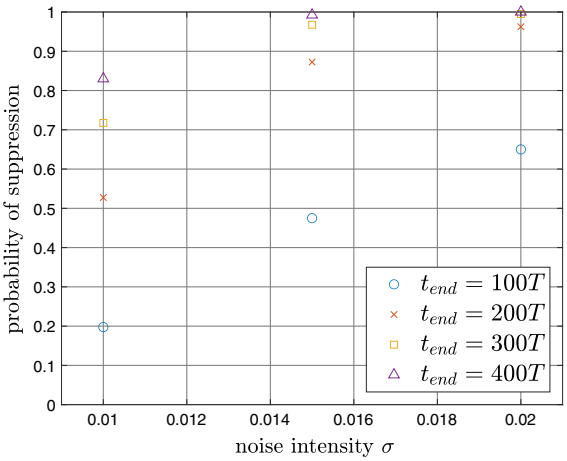

Fig. 7 Probability of suppression of the energy localization: Although for shorter noise application times, the probability of suppressing localization is lower for low noise intensities (e.g., $\sigma = 0.01$), for longer duration, the probability converges to 1 for all tested noise levels

flow through the oscillators, and the localized mode is more sensitive to perturbations. Therefore, it is harder to sustain a localized mode for systems with stronger coupling. In addition, the localization is stronger for systems with weaker coupling in the sense that the amplitude ratio of the localization center to the neighboring oscillators is larger. The effect of nonlinear coupling has also been studied [19], where it is shown that the addition of cubic coupling makes the energy localization weaker. In order to explore the effects of coupling on systems with noise, three scenarios are investigated: (1) the uncoupled system, (2) the linearly coupled array, and (3) the array with both linear coupling and cubic coupling.

3.2.1 Uncoupled system ($k_c = 0$ and $k_{c3} = 0$)

For the uncoupled system ($k_c = 0$), each individual oscillator can be treated as a single oscillator, which oscillates in either the low-amplitude or a high-amplitude response depending on the initial conditions. From previous studies in the authors' group, it is known that Gaussian noise can be used to induce transitions between the two solution branches [8,20]. In search of a practical minimum noise to initiate these transitions, the single oscillator behavior is studied under various noise intensities. For each noise level, one hundred responses are simulated until the transition from the high-amplitude orbit to the low-amplitude orbit starts, and the transition times are recorded. The simulations were truncated, if no transition to the ULA mode was

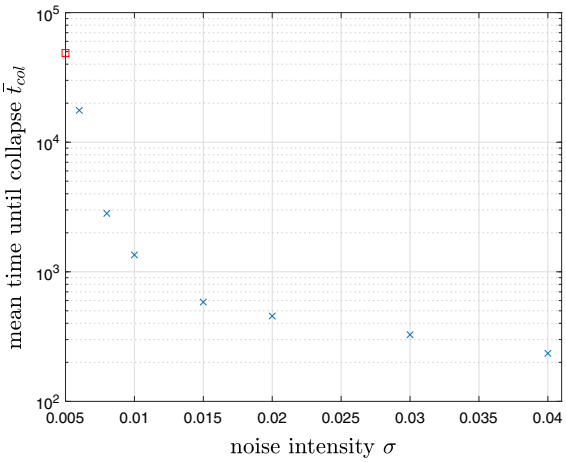

Fig. 8 The average transition time from the high-amplitude response to low-amplitude response for various noise levels ($F_0 = 0.0126$ and $\omega = 1.25$). For $\sigma = 0.005$, the mean transition time is only calculated for realizations where a transition was observed (52 out of 100 samples)

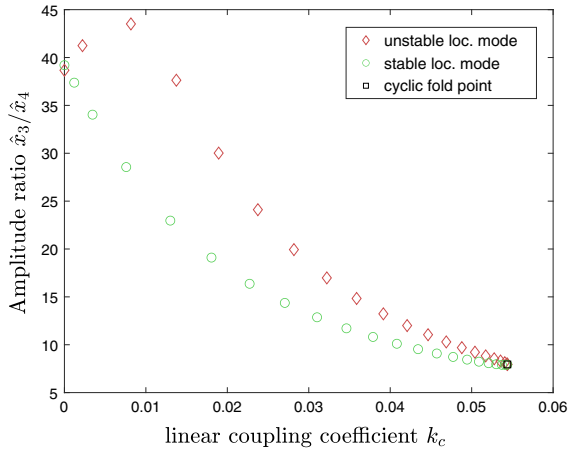

Fig. 9 Amplitude ratio as a measure for localization for varying strength of linear coupling spring coefficient k_c

observed after $2 \cdot 10^4$ periods. The average times ($\bar{t}_{\text{col}}$) for transitions are shown in Fig. 8.

For decreasing noise levels $\bar{t}_{\text{col}}$ increases dramatically. Indeed, according to large deviation theory (e.g., Freidlin and Wentzell [16]), for small noise intensities the mean escape time increases exponentially with decreasing noise intensity σ. Moreover, often the escape times are concentrated in a small band close to the mean value t_{avg}. Thus, this theory also confirms that the likelihood of observing an escape within a fixed time span for small noise intensities is very slim. For $\sigma = 0.005$, about half of the realizations have not transitioned to the ULA mode within $2 \cdot 10^4$ periods[1]. Due to the incomplete suppression of localization at $\sigma = 0.005$, the value $\sigma = 0.006$ can thus be accepted as a practical minimum noise limit for the specified excitation level ($F = 0.0126$).

3.2.2 Linear coupling ($k_c > 0$ and $k_{c3} = 0$)

First, the effect of the linear coupling on localization is studied. To this end, the continuation of the deterministic localized mode is computed for increasing linear coupling stiffness coefficient k_c with the automated numerical continuation package COCO [12]. As a measure of localization, the amplitude ratio of the localization center and its neighboring oscillator $\hat{x}_3/\hat{x}_4$ is shown in Fig. 9. For increasing strength of coupling coefficient k_c the localization decreases, which agrees with [18]. Moreover, in Fig. 9, there is a critical value $k_c^{\text{crit}} \approx 0.54$ at which the localized mode folds over the linear coupling coefficient k_c. Thus, for values of k_c larger than k_c^{crit}, the localized mode ceases to exist. In summary, for increasing coupling coefficients the localized mode not only "delocalizes"; that is, the corresponding amplitude ratio decreases, and further, for large enough k_c values, the localized mode does not exist.

Close to the fold point, in Fig. 9, one can note a change of stability of the localized mode; that is, a cyclic-fold bifurcation [11] of the stable periodic orbit is observed. It is of interest to note that the other merging periodic orbit is the continuation of an unstable localized mode. More specifically, it is the continuation of the unstable localized mode where in the uncoupled or anti-continuum limit ($k_c = 0$) the third mass moves along the unstable periodic orbit with high energy and the other masses are at the stable low amplitude orbit. The bifurcation scenario depicted in Fig. 9 is an example of a classic symmetry breaking bifurcation (e.g., [11,21,22]), induced by the symmetry breaking parameter k_c.

In Fig. 9, localization is found to be stronger for lower coupling. Thus, in the light of the authors' previous studies, one can suggest that suppressing energy

[1] The average over the transitioned samples is included in Fig. 8 for comparison. Since many samples have been discarded, this mean collapse time at $\sigma = 0.005$ is not completely equivalent to the other transition times with $\sigma > 0.005$.

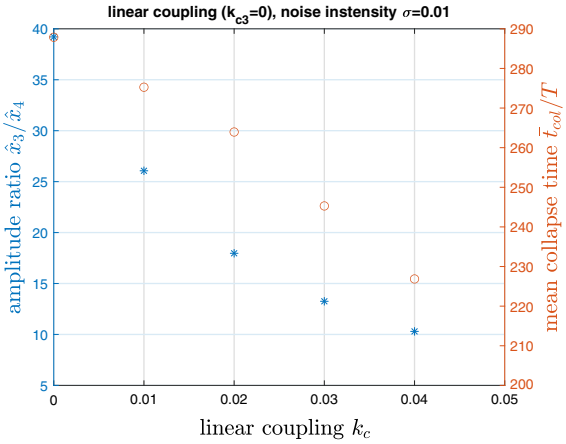

Fig. 10 Mean time necessary to suppress localization for noise intensity $\sigma = 0.01$

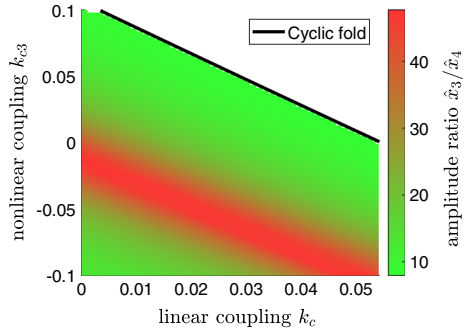

Fig. 11 Amplitude ratio $\hat{x}_3/\hat{x}_4$ for various strengths of linear coupling stiffness and nonlinear coupling stiffness

localization through noise perturbations would be easier for systems with higher coupling. To verify this hypothesis, the mean collapse time; that is, the average duration for trajectories launched at the localized mode to collapse to the ULA mode, is computed for various linear coupling coefficients k_c and the constant noise intensity $\sigma = 0.01$. The average is taken over 10^3 samples. In Fig. 10, the authors show the mean time necessary to suppress energy localization is higher for systems with smaller coupling. Therefore, one can conclude that the energy exchange between the oscillators makes it significantly easier for the noise to suppress energy localizations.

3.2.3 *Linear coupling and nonlinear coupling ($k_c > 0$ and $k_{c3} \neq 0$)*

In addition to the linear coupling, nonlinear coupling may exist in micro-resonator arrays [23] and systems with fluid coupling [24]. In order to study suppression of energy localization in these systems, and observe the effect of nonlinear coupling on the minimum noise intensity, a system with cubic coupling in addition to the linear coupling is also considered. The equations of motion for the coupled oscillator array can be written as

$$\ddot{x}_n + c\dot{x}_n + k_1 x_n + k_3 x_n^3 + f_c(x_n) = F_0 \cos(\omega t) + \sigma \dot{W}(t), \quad (5)$$

for $n = 1, 2, \ldots N$, where it is recalled that the f_c is the coupling spring force with $f_c(x_n) = k_c(2x_n - x_{n-1} - x_{n+1}) + k_{c3}[(x_n - x_{n+1})^3 + (x_n - x_{n-1})^3]$ for $1 < n < N$, $f_c(x_1) = k_c(2x_1 - x_N - x_2) + k_{c3}[(x_1 - x_2)^3 + (x_1 - x_N)^3]$ and $f_c(x_N) = k_c(2x_N - x_{N-1} - x_1) + k_{c3}[(x_N - x_1)^3 + (x_N - x_{N-1})^3]$.

As pointed out in the authors' earlier studies, initiating and sustaining the energy localization is harder for systems with a cubic coupling [19]. To confirm these observations for the cyclic system, the localized mode is computed for various combinations of linear and nonlinear coupling spring coefficients (k_3 and k_{c3}). As a representative result, in Fig. 11, the authors show the amplitude ratio as a measure of localization. The case of only linear coupling; that is, the line $k_{c3} = 0$, is equivalently shown in Fig. 9. For hardening coupling springs ($k_{c3} > 0$), the localization level is found to decrease with increase in k_{c3} until the localized mode undergoes a cyclic fold bifurcation and ceases to exist after the bifurcation. This behavior is analogous to what was observed in the case of a system with purely linear coupling that was discussed in Sect. 3.2.1.

For softening springs ($k_{c3} < 0$), interestingly, as shown in Fig. 9, the authors find a qualitatively different trend. As one decreases the strength of nonlinear spring coefficient below zero, one can actually increase the localization level until a value similar to the uncoupled limit is reached (red areas in Fig. 11). After this maximum is reached, the amplitude ratio drops again, indicating a "delocalization" trend of the localized mode. Contrary to the hardening case and linear case, no cyclic fold points were found for softening nonlinearities in the investigated parameter range.

Repeating the study of the correlation between the amplitude ratio $\hat{x}_3/\hat{x}_4$, a deterministic measure for

localization, and the average collapse time from the previous section for various nonlinear coupling coefficients, the authors obtain Fig. 12. Once again the average taken is over 10^3 samples and the noise intensity is kept constant at $\sigma = 0.01$. The trend of decreasing mean collapse time with decreasing amplitude ratio observed for linear coupling is confirmed for hardening springs $k_{c3} > 0$ (cf. the left plot in Fig. 12 for $k_{c3} > 0$). For softening nonlinearities, this relationship, however, cannot be confirmed. The mean time to collapse can actually increase for decreasing amplitude ratio. Thus, relying on the amplitude ratio as a single indicator to quantify the robustness of localization with respect to noise can be misleading.

Overall, the fundamental differences between softening ($k_{c3} < 0$) and hardening springs ($k_{c3} > 0$) from the deterministic picture in Fig. 11 carry over to the stochastic setting shown in Fig. 12. To understand and uncover the causes of these differences in the stochastic case, a global analysis is required. However, the available numerical analysis tools for stochastic dynamical systems are often limited to single degree of freedom systems [25].

3.3 Suppression of energy localization in large arrays

Exploring an array's response under noise, and finding the minimum noise intensity that can initiate the transitions from the localized mode to the ULA mode require analyzing the system behavior under hundreds of different noise vectors through Monte Carlo simulations. Although feasible for small arrays (e.g., with 6 oscillators), these simulations can be computationally expensive as the number of oscillators in the system grows. Finding the similarities between the responses of small arrays and large arrays can enable modeling simplifications, and reduce the cost of these investigations.

For arrays with low coupling, the localization center is directly affected by its immediate neighbors, and the influence of other oscillators on the localization amplitude is much smaller. The authors' previous work has shown that one can approximate the amplitude profile near the localization by considering only the localization center and its two immediate neighbors [5]. In order to explore if simulating only a few oscillators is sufficient to capture the behavior of energy localization in large arrays subjected to noise, the following study is conducted. Three arrays with different numbers of oscillators are considered: a six-oscillator array, a ten-oscillator array, and a twenty-oscillator array. Additionally, the uncoupled or anti-continuum limit is included. All the arrays are composed of identical oscillators and the inter-oscillator coupling is uniform with $k_c = 0.04$. All arrays are then excited with the same exact noise vector with intensity $\sigma = 0.01$ in addition to the harmonic forcing. The initial condition is selected at the localized mode with the energy localized at the third oscillator.

The time responses of the arrays are shown in Fig. 13. In cases with 6, 10, and 20 oscillators, the amplitude of the third oscillator starts dropping at the same time (around $t = 600$ s), and the time response appears to be the same for the localization center (i.e., third oscillator). For the uncoupled limit, however, the collapse from the localized mode to the ULA mode starts not only significantly later (at around $t = 1000$ s) but also the transition is less rapid. Thus, although in all of the depicted time histories a suppression of localization is observed, it is inferred that the cyclic configuration with a few number of oscillators (e.g., six) is more suitable to mimic the behavior of a large oscillator arrays than the more trivial uncoupled limit.

A phenomenological explanation for why the transitions from the localized mode to the ULA mode in larger cyclic arrays can be accurately mimicked by an array with fewer oscillators is as follows. During the simulations depicted in Fig. 13, it was observed that the displacements and speeds of the masses far away from the localization center are almost identical, although this symmetry is perturbed by the linear stiffness coupling k_c. More specifically, $x_j \approx x_i$ and $\dot{x}_i \approx \dot{x}_i$ holds, where this approximation becomes more accurate the more the integers j and i differ from three; that is, the localization center. Actively enforcing such a behavior, one can propose the model order reduction depicted in Fig. 14. Of course, an in-depth analysis for deriving the observed similarity rather than enforcing it would be preferable to deduce a reliable reduced order model. However, at a phenomenological level, Fig. 14 can be used to explain the observed similarities in the responses of small ($N = 6$) and large ($N = 20$) arrays.

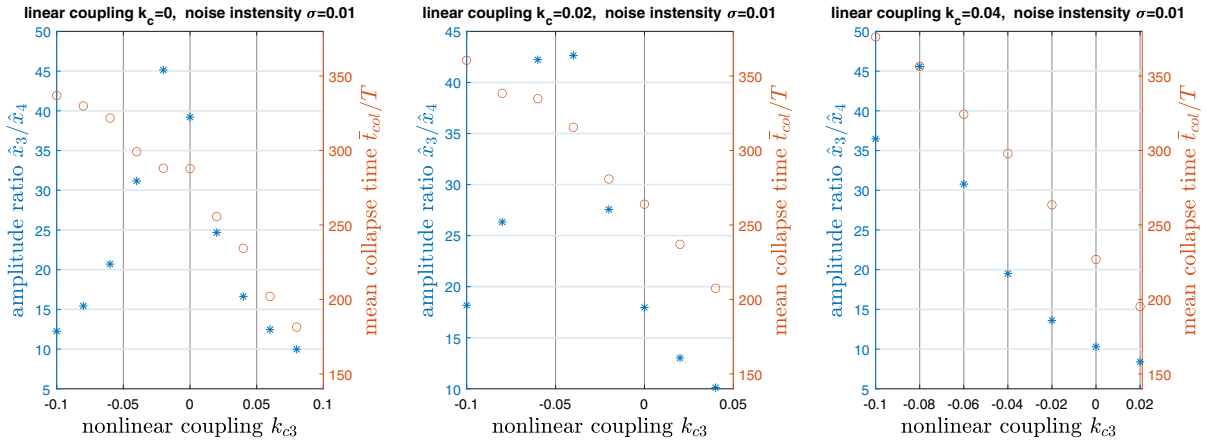

Fig. 12 Mean time necessary to destroy localization for noise intensity $\sigma = 0.01$ and different strengths of linear coupling stiffness and nonlinear stiffness coupling

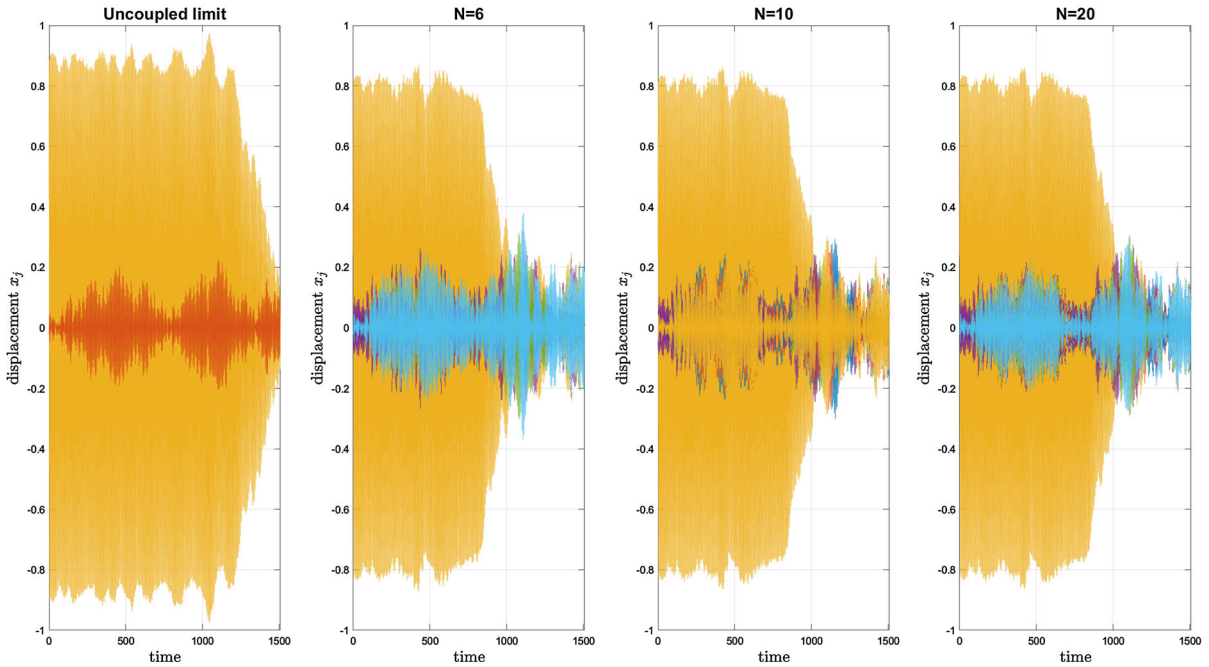

Fig. 13 Time responses for an array with $k_c = 0.04$, N =1, 6, 10 and 20 oscillators subjected to the same noise vector with the intensity $\sigma = 0.01$

3.4 Dynamics with non-Gaussian noise

The assumption of Gaussian white noise is the prevalent assumption in studies of random vibrations. One reason is the well developed mathematical basis. In reality, however, a stochastic excitation will be non-Gaussian, since Gaussian white noise has infinite energy content and hence is not physical. To investigate the effects of non-Gaussian noise models, pink noise is considered as an example. The spectral power density of the pink noise is reciprocal of the frequency f. Hence, it is also labeled as $1/f$-noise or Flicker noise. Amongst others, it has been documented in electrical circuits and metals [26] as well as in natural phenomena such as ocean currents and astronomical time series [27]. The equations of motion of the cyclic oscillator array (4), driven by

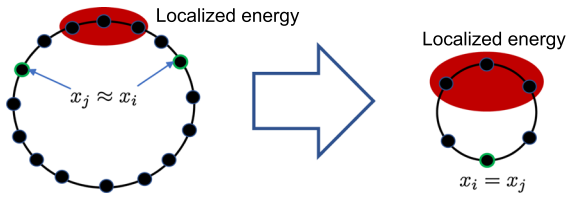

Fig. 14 Phenomenological model order reduction to explain the similarities between array with low and high number of oscillators

the pink noise process W_p is given by

$$\begin{aligned} dx_{n1} &= x_{n2}dt, \\ dx_{n2} &= (F_0\cos(\omega t) - cx_{n2} - k_1x_{n1} - k_3x_{n1}^3 \\ &\quad - f_c(x_{n1}))dt + \sigma dW_p. \end{aligned} \tag{6}$$

There are numerous approaches to generate pink noise; for example, filtering white noise [28], a Green's function [27] approach or constructing this noise in the frequency domain [29]. Once a realization pink noise is created, one can straightforwardly replace the (pseudo-) random number generator in the Euler-Maruyama scheme with the pink noise process. Although the Euler-Maruyama scheme is developed to approximate stochastic integrals where the noise arises from the standard Wiener process [13], this practical approach can be justified. As with many other noise models, pink noise can be obtained by filtering white noise appropriately; that is, it can be obtained as a solution of a filter differential equation of the form

$$\begin{aligned} dW_p &= f(\mathbf{z},t) + b(\mathbf{z},t)dW, \\ d\mathbf{z} &= \mathbf{f}_z(\mathbf{z},t) + \mathbf{b}_z(\mathbf{z},t)dW, \end{aligned} \tag{7}$$

where the vector $\mathbf{z}$ denotes internal states and $f(\mathbf{z},t)$, $b(\mathbf{z},t)$, $\mathbf{f}_z(\mathbf{z},t)$, and $\mathbf{b}_z(\mathbf{z},t)$ are appropriately chosen, possibly nonlinear and time varying, functions. A standard approach to handle system (6) driven by the filtered Gaussian white noise (7) is to extend the state space to include the filter differential equation in the dynamical system (e.g., [30]). Then, one extends the state space to include not only the positions x_n and velocities $\dot{x}_n$ but also the pink noise variable W_p and the internal states $\mathbf{z}$. In this setting one obtains a dynamical system driven by white noise. Thus, results derived for the standard Wiener process apply for the extended dynamical system. Now, one can skip the step of extending the phase space, argue that for each time step the filter equations have already been solved by the built in noise generator and hence it can be included directly into the Euler-Maruyama scheme. Therefore, the sound mathematical basis , most notably the convergence results, of the Euler–Maruyama scheme (e.g., [13]) carry over to non-Gaussian noise case; that is, filtered white noise.

In Fig. 15, the authors show responses of a cyclic oscillator array with a linear coupling spring $k_c = 0.04$. The pink noise was generated with the readily available filter from reference [28]. For this specific realization, the localization was suppressed for both noise models, whereby the collapse occurred earlier in the white noise (briefly after $t = 200$ s) case compared to the pink noise case (slightly before $t = 500$ s).

To check whether the difference observed in Fig. 15 is statistically significant, responses of the cyclic array are computed for one hundred different realizations for each noise model and the intensity is increased to $\sigma = 0.02$. The resulting histogram is shown in Fig. 16. Both distributions are almost identical and thus the observed difference in the escape time in Fig. 15 can be said to be statistically irrelevant. Thus, it can be noted that the localization suppression through white noise observed in the preceding sections also extends to more realistic noise models such as pink noise. While in the specific case investigated even the escape times distribution of white noise and pink noise match, it is generally expected that with different noise models, one will have a differing impact on the dynamics of nonlinear mechanical systems such as oscillator arrays.

4 Concluding remarks

In this work, effects of noise on energy localization in a circular array of coupled nonlinear oscillators have been investigated. The considered system is composed of multiple weakly coupled Duffing oscillators with periodic boundary conditions. When excited with a harmonic forcing at a certain level, the system exhibits the energy localization phenomenon, where one of the oscillators has a significantly higher amplitude compared to the other ones. It is shown that Gaussian noise can perturb the system from this localized mode, and drive the system response to a ULA mode. Moreover, it is observed that the likelihood of successful localization suppression as well as the time necessary to destroy energy localization by noise drops significantly with decreasing noise intensity. Thus, one can find a

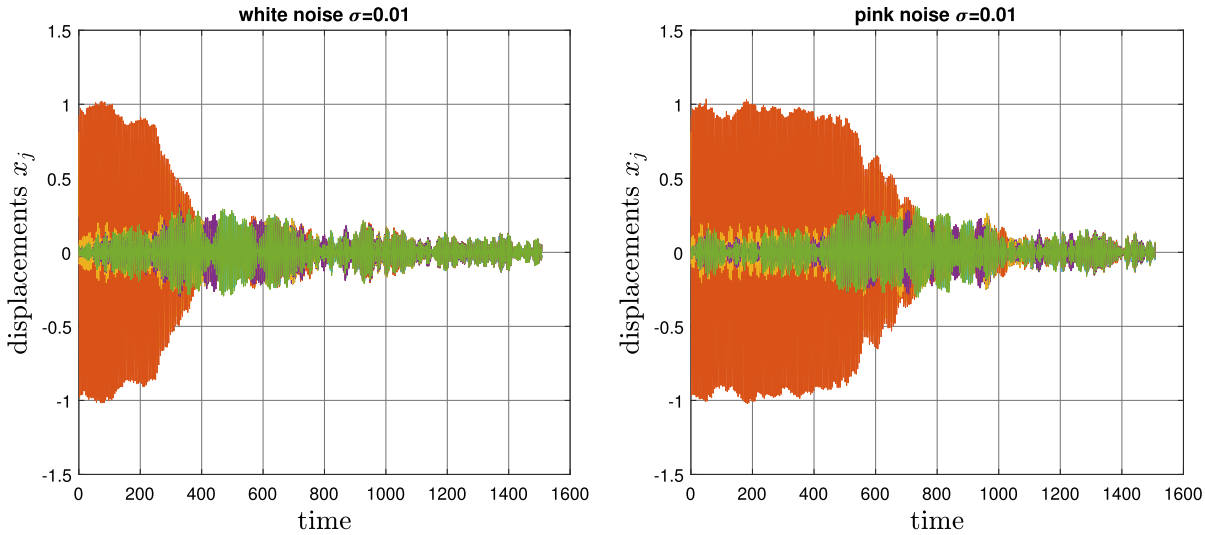

Fig. 15 Comparison of responses of an oscillator array ($k_c = 0.04$) excited by white noise and pink noise

minimum noise level for successful localization suppression.

Subsequently, the dependence of the coupling between the oscillators on the robustness of localization with respect to noise has been investigated. With increasing linear and nonlinear coupling of hardening type, the localized mode is found to be more sensitive to noise. For softening nonlinear coupling, however, the average time to suppress localization actually is found to increase.

A comparison between the six-oscillator cyclic case and higher dimensional arrays revealed no fundamental differences for the noise induced transition from the localized mode to the ULA mode. This fact indicates that the obtained results remain valid for higher dimensional systems. Moreover, based on the authors' observations, a phenomenological reduced order modelling is proposed to model the localization center and a few adjacent neighbors. This simplified model was found to be sufficient to understand the system behavior in this study. In a similar spirit, no essential differences have been observed when the Gaussian white noise is replaced by more realistic noise models such as pink noise. This finding suggests that discoveries based on non-physical Gaussian white noise indeed have a relevance for system behavior with realistic noise models.

The authors' studies with softening coupling spring stiffness remains a first step towards an largely unexplored area. In the same vein, the cases with non-

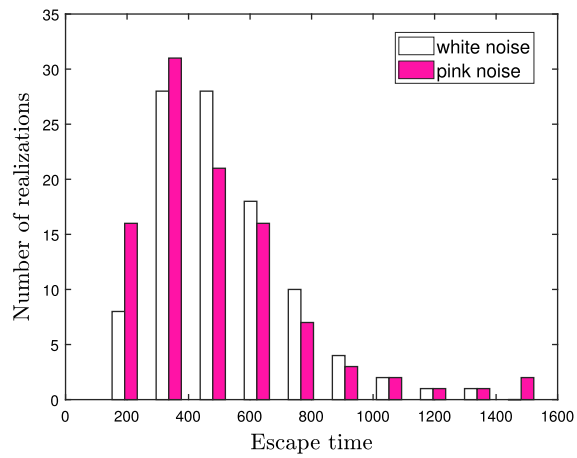

Fig. 16 Histogram of the escape times of the oscillator array ($k_c = 0.04$) excited by white noise and pink noise (sample size = 100)

Gaussian noise should be considered as an initial foray into non-Gaussian noise influenced dynamics. Both aspects call for more fundamental and systematic future work. Furthermore, it is desirable to put the reduced order modelling proposed in Fig. 14 on a firmer footing by carrying out an extensive numerical analysis and/or an analytical treatment.

Currently, the authors are also working on constructing a physical circular array to carry out experiments and enrich the numerical studies with empirical observations. Such experiments can also shed light into the

question whether findings based on Gaussian white noise are of relevance to practical systems. Furthermore, such experiments follow as extensions of earlier experimental investigations on localized modes in deterministic systems [9,31,32] towards the stochastic, and hence, a more realistic setting.

Although, the methods and observations in this work have been provided in the context of circular oscillator arrays, it is believed that this work is also relevant to arrays of oscillators arranged in-line configuration. A fundamental assessment of the impact of different boundary conditions remains a future research topic.

Acknowledgements The authors are grateful for the support received from the U.S. National Science Foundation, through Grant CMMI-1760366.

Data Availability Statement Data used in this work are available as time series data and results provided within the manuscript.

Declarations

Conflict of interest The authors declare that they have no conflict of interest.

References

1. He, Z., Epureanu, B.I., Pierre, C.: Parametric study of the aeroelastic response of mistuned bladed disks. Comput. Struct. **85**(11–14), 852–865 (2007)
2. Sievers, A.J., Takeno, S.: Intrinsic localized modes in anharmonic crystals. Phys. Rev. Lett. **61**(8), 970 (1988)
3. Perkins, E., Chabalko, C., Balachandran, B.: Noise-influenced transient energy localization in an oscillator array. Nonlinear Theory Appl. IEICE **4**(3), 232–243 (2013)
4. Vakais, A.F., Cetinkaya, C.: Mode localization in a class of multidegree-of-freedom nonlinear systems with cyclic symmetry. SIAM J. Appl. Math. **53**(1), 265–282 (1993)
5. Dick, A.J., Balachandran, B., Mote, C.D., Jr.: Intrinsic localized modes in microresonator arrays and their relationship to nonlinear vibration modes. Nonlinear Dyn. **54**(1–2), 13–29 (2008)
6. Dauxois, T., Peyrard, M.: Energy localization in nonlinear lattices. Phys. Rev. Lett. **70**(25), 3935 (1993)
7. Papangelo, A., Fontanela, F., Grolet, A., Ciavarella, M., Hoffmann, N.: Multistability and localization in forced cyclic symmetric structures modelled by weakly-coupled duffing oscillators. J. Sound Vib. **440**, 202–211 (2019)
8. Agarwal, V., Zheng, X., Balachandran, B.: Influence of noise on frequency responses of softening duffing oscillators. Phys. Lett. A **382**(46), 3355–3364 (2018)
9. Perkins, E., Kimura, M., Hikihara, T., Balachandran, B.: Effects of noise on symmetric intrinsic localized modes. Nonlinear Dyn. **85**(1), 333–341 (2016)
10. Marin, J.L., Aubry, S.: Breathers in nonlinear lattices: numerical calculation from the anticontinuous limit. Nonlinearity **9**(6), 1501 (1996)
11. Nayfeh, A.H., Balachandran, B.: Applied Nonlinear Dynamics: Analytical, Computational, and Experimental Methods. Wiley, Hoboken (2008)
12. Dankowicz, H., Schilder, F.: Recipes for continuation. SIAM (2013)
13. Kloeden, P. E., Platen, E.: Numerical solution of stochastic differential equations. Applications of mathematics 23. Springer, Berlin [etc, (3rd corrected printing) edition, (1999)
14. Oksendal, B.: Stochastic Differential Equations: an Introduction with Applications. Springer, Berlin (2013)
15. Higham, D.J.: An algorithmic introduction to numerical simulation of stochastic differential equations. SIAM Rev. **43**(3), 525–546 (2001)
16. Freidlin, M. I., Wentzell, A. D.: Random perturbations. In: Random Perturbations of Dynamical Systems, pages 15–43. Springer, (1998)
17. Matkowsky, B.J., Schuss, Z.: The exit problem for randomly perturbed dynamical systems. SIAM J. Appl. Math. **33**(2), 365–382 (1977)
18. Dick, A.J., Balachandran, B., Mote, C.D., Jr.: Localization in microresonator arrays: influence of natural frequency tuning. J. Comput. Nonlinear Dyn. **5**(1), 011002 (2010)
19. Balachandran, B., Perkins, E., Fitzgerald, T.: Response localization in micro-scale oscillator arrays: influence of cubic coupling nonlinearities. Int. J. Dyn. Control **3**(2), 183–188 (2015)
20. Cilenti, L., Balachandran, B.: Transient probability in basins of noise influenced responses of mono and coupled duffing oscillators. Chaos: Interdiscip. J. Nonlinear Sci. **31**(6), 063117 (2021)
21. Golubitsky, M., Stewart, I., Schaeffer, David G.: Singularities and Groups in Bifurcation Theory: Volume II. volume 69. Springer Science & Business Media (2012)
22. Crawford, J.D., Knobloch, E.: Symmetry and symmetry-breaking bifurcations in fluid dynamics. Annu. Rev. Fluid Mech. **23**(1), 341–387 (1991)
23. Rhoads, J.F., Shaw, S.W., Turner, K.L.: Nonlinear dynamics and its applications in micro-and nanoresonators. J. Dyn. Syst. Measurement Control **132**(3), 034001 (2010)
24. Amabili, M., Païdoussis, M.P.: Review of studies on geometrically nonlinear vibrations and dynamics of circular cylindrical shells and panels, with and without fluid-structure interaction. Appl. Mech. Rev. **56**(4), 349–381 (2003)
25. Masud, A., Bergman, L. A.: Solution of the four dimensional fokker-planck equation: Still a challenge. In: Icossar. volume 2005, pages 1911–1916. Citeseer, (2005)
26. Kogan, S.: Electronic Noise and Fluctuations in Solids. Cambridge University Press, Cambridge (2008)
27. Press, W.H.: Flicker noises in astronomy and elsewhere. Comments Astrophys. **7**, 103–119 (1978)
28. Smith, J. O.: Mathematics of the discrete Fourier transform (DFT): with audio applications. Julius Smith, (2007)
29. Timmer, J., Koenig, M.: On generating power law noise. Astron. Astrophys. **300**, 707 (1995)
30. Caughey, T.K.: Nonlinear theory of random vibrations. Adv. Appl. Mech. **11**, 209–253 (1971)

31. King, M.E., Aubrecht, J., Vakakis, A.F.: Experimental study of steady-state localization in coupled beams with active nonlinearities. J. Nonlinear Sci. **5**(6), 485–502 (1995)
32. Niedergesaß, B., Papangelo, A., Grolet, A., Vizzaccaro, A., Fontanela, F., Salles, L., Sievers, A., Hoffmann, N.: Experimental observations of nonlinear vibration localization in a cyclic chain of weakly coupled nonlinear oscillators. J. Sound Vib. **497**, 115952 (2021)